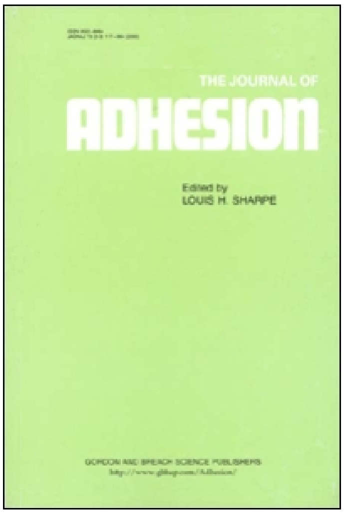

The Journal of Adhesion
Publication details, including instructions for authors and subscription information:
http://www.informaworld.com/smpp/title~content=t713453635

Environmental Failure of Structural Adhesive Joints

R. A. Gledhill[a]; A. J. Kinloch[a]
[a] Ministry of Defence Procurement Executive, Explosives Research and Development Establishment, Essex, England

To cite this Article Gledhill, R. A. and Kinloch, A. J.(1974) 'Environmental Failure of Structural Adhesive Joints', The Journal of Adhesion, 6: 4, 315 — 330

To link to this Article: DOI: 10.1080/00218467408075035

URL: http://dx.doi.org/10.1080/00218467408075035

J. Adhesion, 1974, Vol. 6, pp. 315–330

Printed in Scotland

Environmental Failure of Structural Adhesive Joints

R. A. GLEDHILL and A. J. KINLOCH

Ministry of Defence Procurement Executive, Explosives Research and Development Establishment, Waltham Abbey, Essex, England

(*Received April 22, 1974*)

The deleterious effect of water on structural adhesive joints has been investigated using joints which consist of mild steel substrates bonded with a simple epoxy adhesive. The mechanisms and kinetics of environmental failure have been identified and the instability of the joints in hostile environments successfully predicted from thermodynamic considerations.

INTRODUCTION

The term "structural" adhesive is commonly applied to a wide range of adhesives which are thermo-setting, possess a high modulus and are used in load-bearing structures. The principal advantages in employing adhesives in structural applications are the high strength to weight ratio of bonded components and the resulting increase in design flexibility. However, a serious limitation frequently encountered in the use of structural adhesives is the deleterious effect moisture has upon the strength of a bonded component, especially when the component is also subjected to conditions of relatively high stress and temperature.

The premature failure of structural joints in moist environments has been appreciated for many years[1, 2] and has been the subject of several review papers.[3, 4, 5] However, while a considerable wealth of data has been accumulated concerning the behaviour of different adhesives after exposure to various climatic conditions,[6-10] the mechanisms involved in the environmental failure of structural adhesive joints are little understood. This lack of fundamental knowledge has precluded correlations between accelerated and outdoor weathering tests and predictions as to the stability of structural joints exposed to hostile environments. Consequently, the logical selection of materials and techniques to avoid such failure has been severely hindered.

The work described in this paper was conducted in an attempt to identify the mechanisms of environmental failure of joints consisting of mild steel substrates bonded with a simple epoxy adhesive, with particular reference to the thermodynamics and kinetics of the failure process.

Theoretical

The thermodynamic work of adhesion, W_A, required to separate unit area of two phases forming an interface may be related[11] to the surface free energies by the Dupré[11] equation. In the absence of chemisorption and interdiffusion the reversible work of adhesion, W_A, in an inert medium may be expressed by:

$$W_A = \gamma_x + \gamma_y - \gamma_{xy} \tag{1}$$

where γ_x and γ_y are the surface free energies of the two phases and γ_{xy} is the interfacial free energy. In the presence of a wetting liquid (denoted by the suffix 'L'), the work of adhesion, W_{AL}, is:

$$W_{AL} = \gamma_{xL} + \gamma_{yL} - \gamma_{xy} \tag{2}$$

For a typical organic adhesive-metal oxide interface the work of adhesion, W_A, in an inert atmosphere, e.g. dry air,[12] usually has a large positive value, indicating thermodynamic stability of the interface. However, in the presence of a liquid the thermodynamic work of adhesion, W_{AL}, may well have a negative value, indicating that the interface is now unstable and will dissociate. Thus, calculation of the terms W_A and W_{AL} may enable the environmental stability of an interface to be predicted.

The thermodynamic works of adhesion, W_A and W_{AL}, may be calculated by first expressing the interfacial free energy, γ_{xy}, by[13, 14]:

$$\gamma_{xy} = \gamma_x + \gamma_y - 2[(\gamma_x^D \gamma_y^D)^{\frac{1}{2}} + (\gamma_x^P \gamma_y^P)^{\frac{1}{2}}] \tag{3}$$

where γ^D and γ^P are the dispersion and polar free force components of the total surface free energy, γ, respectively and

$$\gamma = \gamma^D + \gamma^P \tag{4}$$

Now substituting for the interfacial free energies in Eqs. (1) and (2) by Eq. (3), and by analogous equations for γ_{xL} and γ_{yL}, yields:

$$W_A = 2[(\gamma_x^D \gamma_y^D)^{\frac{1}{2}} + (\gamma_x^P \gamma_y^P)^{\frac{1}{2}}] \tag{5}$$

and

$$\begin{aligned} W_{AL} = 2[\gamma_L &- (\gamma_x^D \gamma_L^D)^{\frac{1}{2}} - (\gamma_x^P \gamma_L^P)^{\frac{1}{2}} - (\gamma_y^D \gamma_L^D)^{\frac{1}{2}} \\ &- (\gamma_y^P \gamma_L^P)^{\frac{1}{2}} + (\gamma_x^D \gamma_y^D)^{\frac{1}{2}} + (\gamma_x^P \gamma_y^P)^{\frac{1}{2}}]. \end{aligned} \tag{6}$$

The values of the parameters on the right-hand sides of these equations are experimentally accessible and hence the thermodynamic works of adhesion, W_A and W_{AL}, may be calculated.

EXPERIMENTAL

The materials and their characterization

The adhesive employed was a diglycidyl ether of bisphenol A (Epikote '828' epoxy resin supplied by Shell Chemicals Ltd.) mixed with 9.4 mass per cent of a curing agent, tri-2-ethyl hexanoate of 2,4,6 tris(dimethylaminomethyl)phenol (HY 959, supplied by Ciba-Geigy UK Ltd.).

To ascertain the cohesive properties of the adhesive, specimens were cast and then cured at 23°C for 96 hours, followed by 100°C for 1¼ hours and finally 180°C for 2½ hours. Following the cure, the specimens were allowed to cool slowly. The cohesive mechanical properties were determined using dumb-bell shaped specimens having a gauge length of 30 mm and a cross-sectional area of approximately 12 mm^2. These specimens were fractured at 20°C and a strain rate of $1.4 \times 10^{-3}\ s^{-1}$ employing an Instron tensometer. Equilibrium contact angles also were measured at 20°C for various liquids on samples of cast adhesive sheet by means of a travelling microscope fitted with a goniometer attachment.

The substrate was mild steel to specification BS 970, EN3B and was in the form of blocks, 2.54 cm^3. The surface to be bonded was first subjected to a liquid and vapour degreasing bath of trichloroethylene, then grit blasted with 180–220 mesh alumina, then degreased again and finally allowed to air dry in a desiccator.

The structure of the oxide formed on the mild steel surface was ascertained by means of an x-ray diffraction technique. A sample of the oxide to be analysed was scraped from the steel surface and a powder x-ray diffraction pattern obtained using a Debye–Scherrer powder camera.

Joint preparation and testing

Immediately prior to joint preparation the mild steel substrates were treated as described above, adhesive was spread on the treated faces and the two blocks were pressed lightly together to form a coaxial butt joint. Small lengths of copper wire, previously inserted in the adhesive near the centre of the joint, were employed to control the glue line thickness to 0.5 mm (this technique has been shown not to significantly affect the joint strength[15, 16]). To effect cure of the adhesive the joint was subjected to the same time/temperature schedule as described previously.

The joints were then exposed to various environments, namely a control environment of 20°C, 56% R.H. and immersion in distilled water at 20, 40, 60 and 90°C. At intervals joints were removed from the above environments, kept at 20°C, 56% R.H. for about half an hour, and then fractured in tension at 20°C and a strain-rate of $4.0 \times 10^{-2}\ s^{-1}$.

After joint fracture the nature and topography of the joint's fracture surfaces were examined both visually and by scanning electron microscopy. Also, to provide further information as to the locus of joint failure, electron probe microanalysis was employed. Since only the metallic elements usually emit x-rays of sufficient intensities to be readily detectable a tracer, 5 mass % of titanium dioxide, was incorporated in the adhesive prior to joint preparation, and the fracture surfaces were analysed for iron and titanium by means of a Cambridge Instruments Mk 2A microanalyser.

RESULTS

The thermodynamic work of adhesion

The various liquids which were used for the contact angle measurements are shown in Table 1. Also tabulated are the respective values of the dispersion force component, γ_L^D, and the polar force component, γ_L^P, of the total surface free energy, γ_L, of each liquid.[17]

TABLE I

Surface free energies of liquids and contact angles

Liquid	Surface free energy (mJ/m²) γ_L^D	γ_L^P	γ_L	Contact angle on adhesive
Water	22.0	50.2	72.2	74°
Glycerol	34.0	30.0	64.0	57°
Formamide	32.3	26.0	58.3	50°
di-iodomethane	48.5	2.3	50.8	31°
1-bromonaphthalene	44.6	0.0	44.6	10°

The measured contact angles of these liquids on the adhesive are also shown in Table 1 and are the average of at least five individual determinations, the reproducibility being within ±2°.

The surface free energies of the materials were determined from the measured contact angles, θ, and reported values of γ_L^D, γ_L^P and γ_L by using the computational analysis proposed by Kaelbe.[18] In this analysis a pair of simultaneous equations is derived which for two liquids, i and j, on a common solid surface may be written:

$$\left.\begin{aligned} 1 + \cos\theta_i &= \frac{2(\gamma_S^D)^{\frac{1}{2}}(\gamma_L^D)_i^{\frac{1}{2}}}{(\gamma_L)_i} + \frac{2(\gamma_S^P)^{\frac{1}{2}}(\gamma_L^P)_i^{\frac{1}{2}}}{(\gamma_L)_i} \\ 1 + \cos\theta_j &= \text{the same except } j \text{ in place of } i \end{aligned}\right\} \qquad (7)$$

If the values of θ, γ_L^D, γ_L^P and γ_L for the two liquids are known, these equations may be solved to yield the dispersion, γ_S^D, and the polar force, γ_S^P, components of the surface free energy of the solid. The total surface free energy, γ_S, is then simply the sum of these components.

A computer program was written so that the values of γ_S^D, and γ_S^P and γ_S of the adhesive could be evaluated from all dissimilar pair combinations of liquids by the use of Eq. (7). Liquid pairs which contributed linear dependence in the simultaneous solution of Eq. (7) were excluded by the test condition[18, 19] that, for inclusion, liquid pairs must possess an absolute value of $D \geqslant 10$ mJ/m^2, where

$$D = [(\gamma_L^D)_i(\gamma_L^P)_j]^{\frac{1}{2}} - [(\gamma_L^D)_j(\gamma_L^P)_i]^{\frac{1}{2}} \qquad (8)$$

The arithmetical mean values of γ_S^P, γ_S^D and γ_S and the respective standard deviations from the mean, $\pm\delta^D$, $\pm\delta^P$ and $\pm\delta$ calculated for the adhesive are shown in Table 2.

TABLE II

Dispersion and polar force components of the solid surface energy

	Surface free energy (mJ/m^2)		
Solid surface	$\gamma_S^D \pm \delta^D$	$\gamma_S^P \pm \delta^P$	$\gamma_S \pm \delta$
Epoxy adhesive	41.2 ± 2.4	5.0 ± 0.8	46.2 ± 1.6
Ferric Oxide	107	1250	1357

The x-ray diffraction studies indicated that the oxide formed on the freshly prepared mild steel surfaces was ferric oxide, Fe_2O_3, and this is in accord with previous work.[20] Thus, the values of γ_S^D, γ_S^P and γ_S of a ferric oxide surface are also shown in Table 2; the values were obtained from the work of Haskins and Loeser[21] and Eberhart.[22]

The thermodynamic work of adhesion for an epoxy adhesive-ferric oxide interface in an inert medium, W_A, and in water, W_{AL}, may now be deduced from equations (5) and (6). The values of W_A and W_{AL} are 291 mJ/m^2 and -255 mJ/m^2 respectively.

Fracture studies

The dependence of the cohesive breaking stress of the epoxy adhesive on the time for which specimens were exposed to the various environments is shown in Figure 1. (The individual results shown for this and other subsequent fracture measurements are the mean of four replicate tests and the coefficient of variance was 8%.) The cohesive breaking stress of the adhesive was initially 53.2 MN/m^2 and the only significant changes occur after the material has been immersed in water at 90°C. In such an environment the adhesive's breaking stress exhibits a fairly rapid decay.

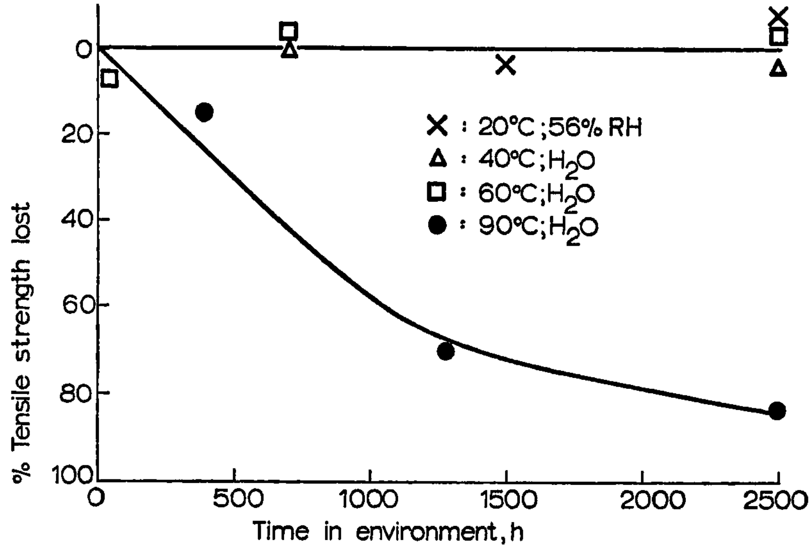

FIGURE 1 Cohesive Breaking Stress of Adhesives vs. Time in Environment.

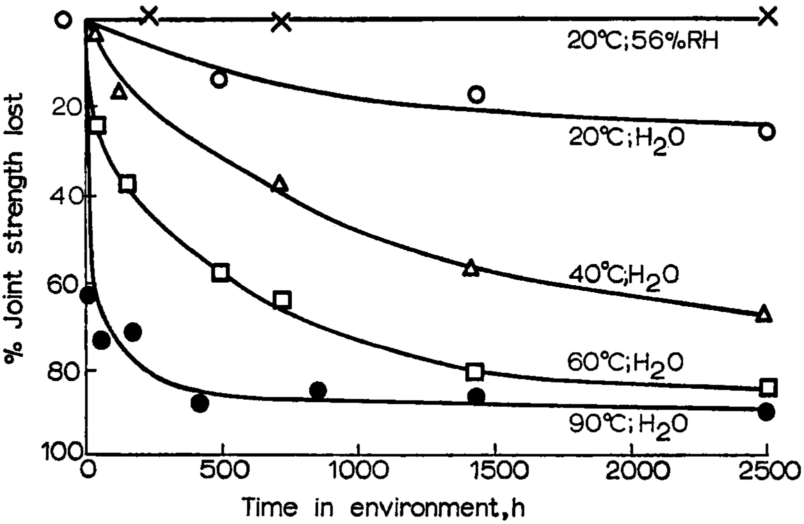

FIGURE 2 Butt Joint Stress *vs.* Time in Environment.

The initial breaking stress of the mild steel-epoxy butt joints was 37.5 MN/m^2 and the change in this parameter as a function of the time the joints were exposed to the various environments, prior to testing at 20°C, is shown in Figure 2. The joints exposed to the control environment of 20°C and 56% R.H. suffered no significant change in joint strength. However, for the joints exposed to the other environments, all of which involved immersion in water, the measured strengths decreased considerably; the higher the immersion temperature, the more rapid was the decay.

To ensure that these observed losses of joint strength were not solely due to the high temperatures employed, joints were exposed to 40°, 60° and 90°C at nominally 0% R.H. No significant losses in joint strength were recorded even after prolonged exposure.

Locus of failure studies

Visual examination of the surfaces of the fractured joints indicated that the initial locus of joint failure was mainly cohesive through the adhesive. For the joints exposed to the control environment there was no significant change in this observed failure pattern. However, for all the joints immersed in water a more complex locus of failure was evident and is illustrated, diagrammatically, in Figure 3.

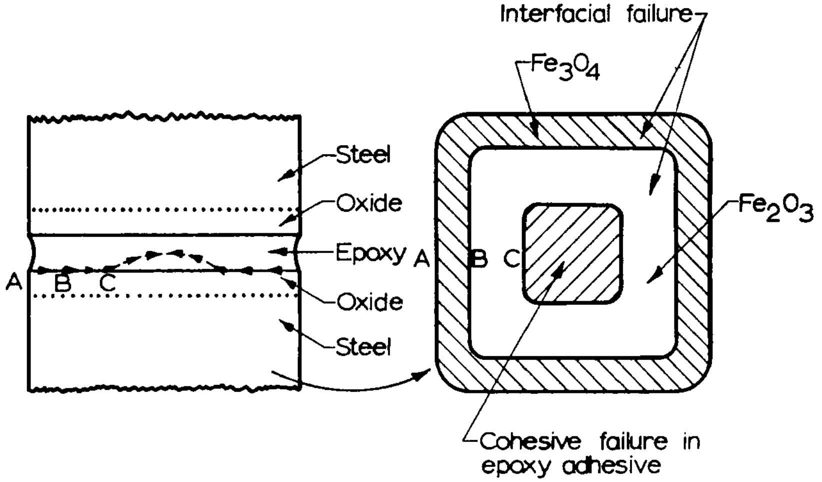

FIGURE 3 Sketch of Locus of Joint Failure after Immersion in Water.

In Figure 3 the locus of joint failure in the central region of the joint is still cohesive through the adhesive. However, from point "A" to "C" apparently interfacial failure occurs, i.e. the fracture path is between the adhesive and metal oxide. Further, as the immersion time is increased this solely interfacial failure region increases at the expense of the cohesive failure region, from the periphery of the joint inwards. The fractional depth of penetration of the interfacial failure region is plotted against the immersion time in Figure 4 and, as may be seen, the rate of ingress of this type of failure pattern is constant at constant temperature but increases as the immersion temperature is increased.

Another distinct feature of this complex failure behaviour was that, usually, only the metal oxide surface in the inner regions of the interfacial failure zone (e.g. points "B" to "C" in Figure 3) resembled that of the freshly prepared oxide surface in possessing a bright, light-grey appearance. In the outer regions (e.g. "A" to "B" in Figure 3) the metal oxide had a dark, almost black, appearance.

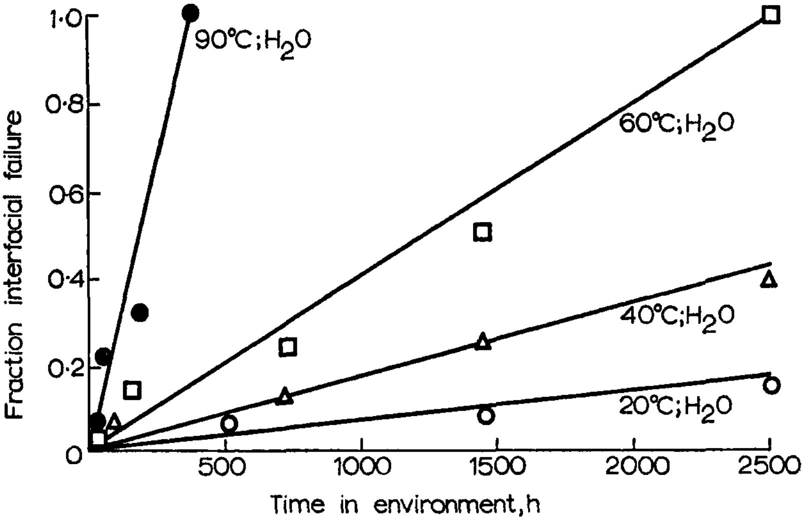

FIGURE 4 Fractional Penetration of Interfacial Failure Region *vs.* Time in Environment.

The rate of advance of this corrosion product on the metal oxide surface was slower than that of the ingress of the interfacial failure region itself but its rate of advance was temperature dependent, as may be seen from Figure 5. There was usually no detectable corrosion of the metal surfaces from those joints exposed to water at 20°C except after 2500 hours when, in some instances, corrosion could just be observed at the edges of the substrate surface.

Examination of the joint fracture surfaces using scanning electron microscopy confirmed the locus of failure behaviour deduced from the visual inspections. In Figure 6 typical scanning micrographs of the metal surface are shown (a) freshly prepared, prior to bonding, (b) in the inner failure region (e.g. an area of the zone bounded by points "B" to "C" in Figure 3), and (c) where the dark corrosion product has formed. As may be seen the surfaces of the substrates are extremely irregular and there are no significant differences in their topographies, indicating that the locus of joint failure is interfacial but providing little information as to the nature of the corrosion product.

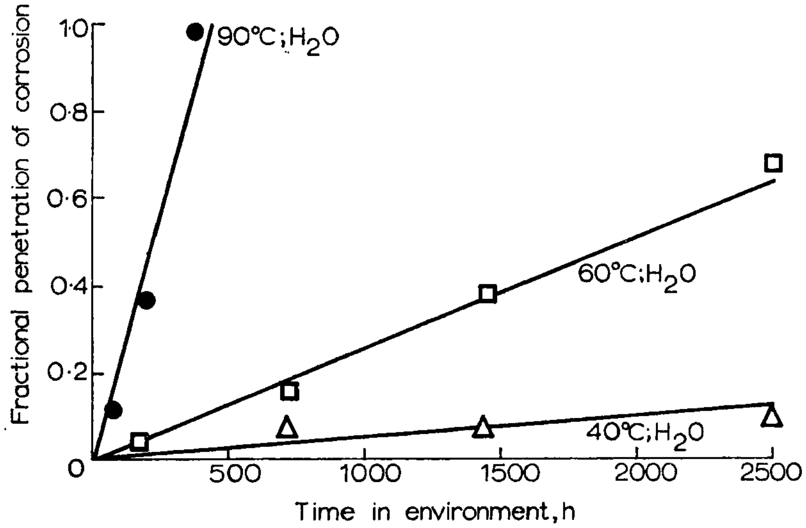

FIGURE 5 Fractional Penetration of Corrosion *vs.* Time in Environment.

This corrosion product was however identified from the x-ray diffraction studies as being mainly composed of magnetite, Fe_3O_4, which, indeed has a dark appearance and is an oxide known to be involved in the corrosion of steel.[23] In the inner interfacial failure region, where the oxide surface was little changed in appearance, the x-ray diffraction studies confirmed that the surface was still mainly composed of ferric oxide.

The locus of joint failure was also ascertained by means of electron probe microanalysis. A tracer, titanium dioxide, was incorporated in the adhesive prior to joint preparation and the fracture surfaces analysed for iron and titanium and compared to the background radiation levels. Some typical results are shown in Table 3 and demonstrate that the joint subjected to the relatively dry environment prior to fracture fails by cohesive fracture through the adhesive. However, if immersed in water, the locus of joint failure progressively becomes interfacial, since there is no significant amount of iron on the adhesive surface or vice versa. These and similar results clearly confirmed the locus of joint failure shown diagrammatically in Figure 3.

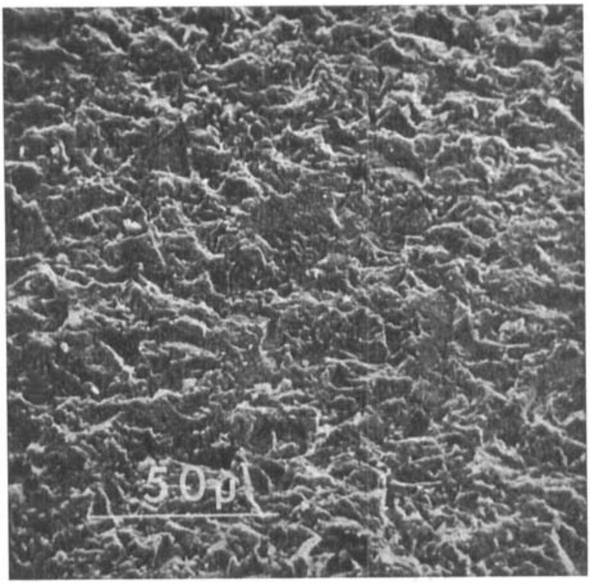

(*a*)

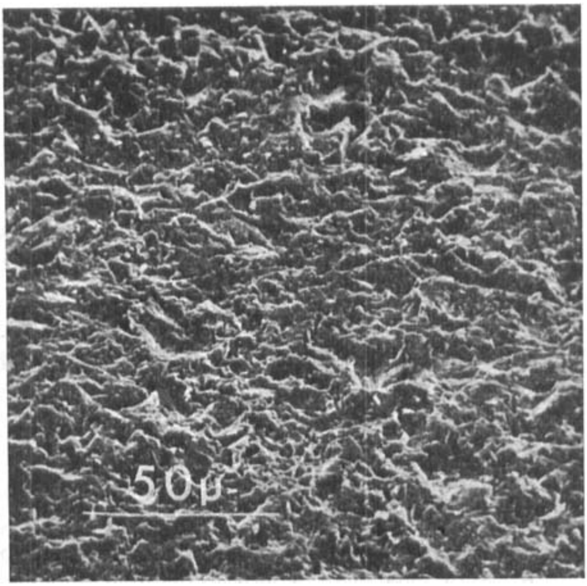

(*b*)

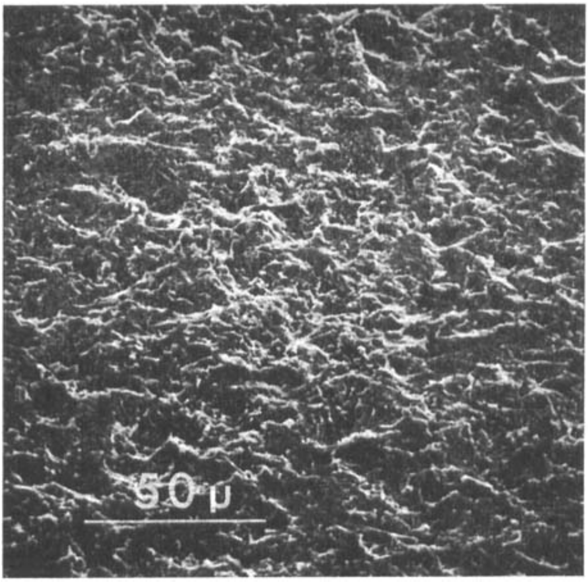

(*c*)

FIGURE 6 Scanning Electron Micrographs of the Substrate's Surface

a) Prior to Bonding

b) In the Interfacial Failure Region after Bonding followed by Fracture

c) In the Interfacial Failure Region after Bonding, Fracture and Corrosion

TABLE III

Results from electron probe microanalysis

Joint environment prior to fracture	Visual surface appearance	Iron analysis[a]			Titanium analysis[a]		
		Analysis (c.p.s.)	Background (c.p.s.)	Difference[b]	Analysis (c.p.s.)	Background (c.p.s.)	Difference[b]
20°C; 56% RH for 2,500 h	Adhesive	1184	1138	NS	9446	280	HS
	Adhesive	1220	1119	NS	2908	175	HS
60°C; H_2O for 2,500 h	Adhesive	7919	7986	NS	3158	2660	HS
	Metallic	7845	1099	HS	266	263	NS

[a] Results shown are mean of six determinations; coefficient of variation ranged from 1 to 10%.

[b] The significance of the differences between "analysis" and "background" counts were determined by using Student's "t" test; NS and HS mean not significant and highly significant respectively.

Discussion

The cohesive breaking stress of the adhesive is not affected by even prolonged immersion in water at temperatures of 20°, 40° and 60°C and this clearly demonstrates that the observed losses of joint strength under these conditions cannot be directly attributed to degradation of the adhesive. When an immersion temperature of 90°C is employed, the cohesive breaking stress decays with time and may be partially responsible for losses of joint strength. An important corollary is that the use of an immersion temperature as high as 90°C to accelerate environmental effects may provide misleading results because a mechanism for joint decay is operative which does not exist at lower temperatures.

These observations strongly suggest that losses in joint strength, after immersion in water, normally result because of the adverse affect of water on the interface, or interphase, rather than on the bulk properties of the adhesive.

For the epoxy-ferric oxide interface the thermodynamic work of adhesion, W_A, is 291 mJ/m^2 and, being positive, the interface is stable in dry environments. This is reflected by the complete retention of strength observed when joints are exposed to conditions of low humidity. However, when there is an adsorbed layer of water at the interface, the thermodynamic work of adhesion becomes W_{AL}, and has a negative value, namely -255 mJ/m^2.

The change from a positive to negative work of adhesion provides a driving force for the displacement of adhesive on the metal oxide surface by water. It is therefore to be expected that if a joint is subjected to a humid environment there will be a progressive encroachment into the joint of debonded interface. This will have the effect of progressively reducing the joint strength and also of progressively changing the locus of failure from cohesive within the adhesive to interfacial between adhesive and substrate. This is exactly what is observed in practice.

The locus of failure studies provide an insight into the kinetics of the displacement mechanism. In Figure 7 the rate of dissociation of the epoxy-ferric oxide interface, deduced from Figure 4, is shown as a function of the immersion temperature in the form of an Arrhenius plot and several interesting features are evident. First, for the three lowest temperatures, a linear correlation exists which yields an activation energy, E_A, for the displacement of adhesive by water of 32 kJ/mol. This value is similar to that for the diffusion of water through an epoxy resin, namely 16 to 38 kJ/mol[24, 25], and suggests that the rate of interface debonding is controlled by the availability of water at the interface governed by diffusion of water probably through the adhesive. The rate of interfacial debonding at an immersion temperature of 90°C is far greater than would be expected from an activation energy of 32 kJ/mol. It is suggested that the main cause for this is that the glass transition temperature, Tg, of the adhesive is 85°C and, at temperatures above this, segmental motions of the polymer chains greatly increase. This permits diffusing species to penetrate far more rapidly than would be predicted from experiments conducted below the Tg. Another factor operative at 90°C is, of course, the degradation of the adhesive which was shown by the measurements of cohesive breaking stress.

The locus of failure studies also enable the role of substrate corrosion in environmental failure to be elucidated. First, the corrosion product, magnetite, was absent from the metal fracture surfaces of joints which were immersed in water at 20°C although under these conditions interfacial debonding was observed and the joint strengths decreased. Secondly, in those instances where corrosion was observed, it occurred after the displacement of adhesive on the metal oxide surface by water (cf. Figures 4 and 5). These observations clearly demonstrate that corrosion of the substrate is not a primary mechanism in the environmental failure of these structural joints but rather a post-failure phenomenon. The rate of corrosion ingress is shown as a function of the immersion temperature, in the form of an Arrhenius plot, in Figure 8. (The maximum possible rate of corrosion ingress being estimated for the 20°C immersion experiments.) The linear correlation yields an activation energy, E_c, for the formation of magnetite of 67 kJ/mol.

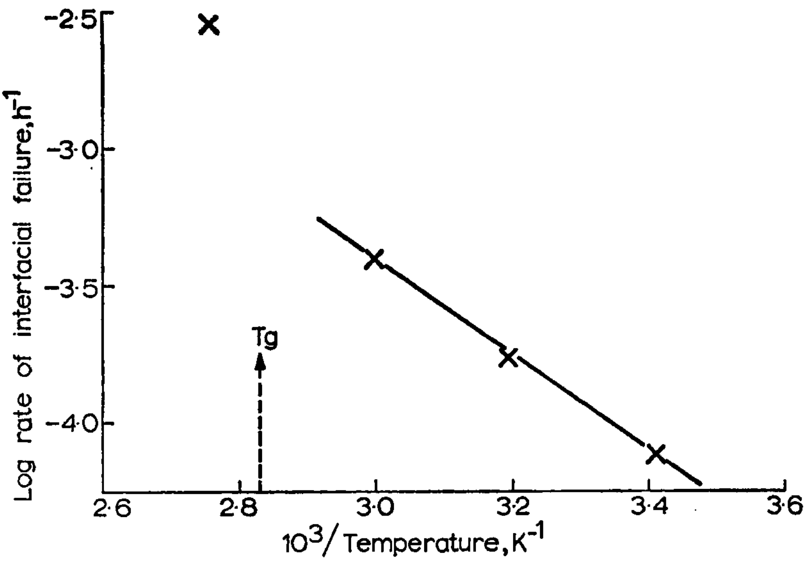

FIGURE 7 Log Rate of Interfacial Failure Penetration *vs.* Reciprocal of the Immersion Temperature.

Finally, having elucidated the mechanics and kinetics of the environmental failure of the joints and established the role of substrate corrosion, it would be of interest and practical importance to quantify the joint strength behaviour upon exposure to a hostile environment. However, this would require a detailed knowledge of the stress distribution in the butt joint geometry and also an analysis which considers several further complicating factors. The first of these is the large-scale internal stresses in the adhesive which arise from shrinkage during cure[26] and from the differential thermal expansions of the adhesive and substrate. Secondly, the epoxy adhesive absorbs water and the equilibrium water content was determined to be between 3 mass % to 7 mass %, depending upon the environment. Whilst swelling of the adhesive will initially tend to counteract stresses arising from thermal shrinkage, swelling stresses may eventually lead to far greater stress concentrations and, hence, reductions in joint strength. Thirdly, the stresses arising from the thermal shrinkage and swelling of the adhesive will be temperature dependent

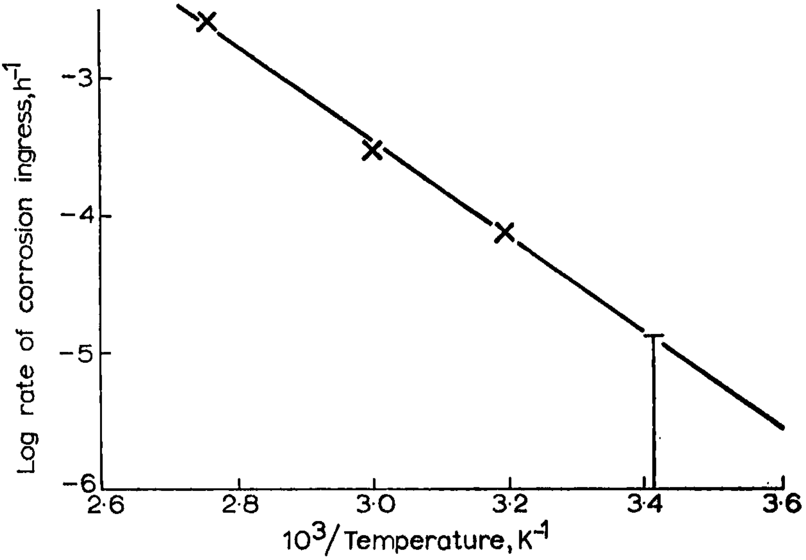

FIGURE 8 Log Rate of Corrosion Ingress *vs.* Reciprocal of the Immersion Temperature.

and, furthermore, at higher temperatures relaxation and flow of the adhesive may partially relieve the internal stresses. It has been shown qualitatively that all these factors may influence the magnitude of the strength of joints[2, 27, 28] and composites[29, 30] during environmental testing but no quantitative data is known to the authors. Therefore, the stability of the epoxy-ferric oxide interface in an environment may be ascertained and the joint strength qualitatively predicted from thermodynamic considerations, but a quantitative assessment is not yet possible.

CONCLUSIONS

Immersion in water has been shown to reduce considerably the strength of structural joints consisting of mild steel substrates bonded with an epoxy adhesive. The mechanism for the environmental failure of these joints is the displacement of adhesive on the metal oxide surface by water and this can be predicted from thermodynamic considerations. The kinetics of this mechanism have been elucidated and are governed by the rate of diffusion of water through the adhesive to the interface. This thermodynamic approach can be employed to predict the stability of any interface in any liquid, providing chemisorption and interdiffusion across the interface are absent. Indeed, thermodynamic considerations predict that the epoxy-ferric oxide interface will be stable in ethanol but dissociate in formamide and this has been experimentally confirmed.[3, 31]

At high environmental temperatures, above the glass transition temperature of the adhesive, the rate of migration of water through the adhesive will be greatly accelerated. In addition, a second mechanism of failure in the form of degradation of the adhesive may become operative. Thus at high temperatures the durability of a joint may be decreased by factors which do not exist at lower temperatures. If therefore may be misleading to deduce the durability of a joint from the results of accelerated testing carried out at temperatures above those which may be encountered during normal use. This is probably one of the reasons for the poor correlations between results from accelerated laboratory testing and outdoor climatic trials.[5]

It has also been established that substrate corrosion is not an operative mechanism in the environmental failure of the joints but, rather, a post-failure phenomenon. Nevertheless, in practical applications such post-failure corrosion could still be of concern since it will weaken the substrate and may cause premature fracture of the bonded component.

The deleterious effect of water on the joint strength and post-failure corrosion of the substrate could both be avoided if the integrity of the interface could be maintained in the presence of moisture. The thermodynamics indicate, however, that if only secondary forces are acting across the interface water will virtually always desorb an organic adhesive from a metal oxide surface. Thus, either water must be prevented from reaching the interface in sufficient concentration to displace the adhesive, or stronger, interfacial forces must be forged which are resistant to rupture by water. This latter requirement emphasises the vital role of the substrate surface treatment, prior to joint preparation, and current research is continuing on surface treatment techniques.

Acknowledgements

The authors would like to thank Mrs. M. Corthine and other colleagues for their assistance with various aspects of the experimental work.

References

1. D. A. Barlow, *The Effect of Dry and Wet Exposure Tests at Elevated Temperatures on the Static Shear Strength of Redux Joints* (ALCAN International Ltd., Banbury, U.K., 1948) Report B-BR-73-48-27.
2. D. J. Falconer, N. C. MacDonald and P. Walker, *Chem. & Ind.*, 1230 (1964).
3. S. Orman and C. Kerr, *Aspects of Adhesion*, **6**, Ed., D. J. Alner (Univ. Press, London 1969). P. 64.
4. W. C. Wake, *Aspects of Adhesion*, **7**, Ed., D. J. Alner & K. W. Allen, (Transcripta Books, London 1973). P. 232.
5. A. J. Kinloch, *Environmental Failure of Structural Adhesive Joints – A Literature Survey* (U.K. Ministry of Defence, Explosives Research and Development Establishment, Waltham Abbey, 1974) Technical Note 95.
6. M. G. D. Hockney, *Effect of Outdoor Exposure on Stressed and Unstressed, Adhesive Bonded Metal-to-Metal Joints, Trial 2 – Two Year Summary* (U.K. Ministry of Defence, Royal Aircraft Establishment, Farnborough, 1972). Report 72100.
7. M. G. D. Hockney, *ibid.*, *Trail 1 – Four Year Summary* (*idem*, 1973) Report 73016.
8. G. F. Carter, *ASTM Special Technical Publication No. 401*, **28**, (1966).
9. R. F. Wegman, *Appl. Polym. Symposia* **19**, 385 (1972).
10. N. J. DeLollis and O. Montoya, *J. Appl. Polym. Sci.* **11**, 983 (1967).
11. G. Salomon, *Adhesion and Adhesives*, Ed., R. Houwink and G. Salomon (Elsevier, Amsterdam, 1962). Chap. 1., p. 30.
12. C. Kerr, N. C. MacDonald and S. Orman, *J. Appl. Chem.* **17**, 62 (1967).
13. D. K. Owen and R. C. Wendt, *J. Appl. Polym. Sci.* **13**, 740 (1969).
14. D. H. Kaelble and K. C. Uy, *J. Adhesion* **2**, 50 (1970).
15. R. W. Bryant and W. A. Dukes, *Appl. Poly. Symposia* **3**, 81 (1966).
16. R. W. Bryant and W. A. Dukes, *Brit. J. Appl. Phys.* **16**, 101 (1965).
17. F. M. Fowkes, *Treatise on Adhesion and Adhesives* Ed., R. L. Patrick (Marcel Dekker, New York, 1967). P. 325.
18. D. H. Kaelble, *J. Adhesion* **2**, 66 (1970).
19. E. H. Andrews and A. J. Kinloch, *Proc. Roy. Soc. Lond.* **A332**, 385 (1973).
20. H. A. Miley and U. R. Evans, *J. Chem. Soc.*, 1295 (1937).
21. W. D. Harkins and E. H. Loeser, *J. Chem. Phys.* **18**, 556 (1950).
22. J. G. Eberhart, *Trans. Metal Soc. AIME* **236**, 1362 (1966).
23. U. R. Evans, D. E. Davies and J. N. Agar, *Proc. Roy. Soc.* **A225**, 443 (1954).
24. J. A. Manson and E. H. Chiu, *J. Polym. Sci. Symp. No.* **41**, 95 (1973).
25. J. Bardeleben, *Kunststoffe* **53**, 162 (1963).
26. V. V. Bolotin and K. S. Boktina, *Mech. Polimerov* **192**, (1), 178 (1972).
27. S. Mostovoy and E. J. Ripling, *J. Appl. Polym. Sci.* **15**, 661 (1971).
28. E. J. Ripling, S. Mostovoy and C. Bersch, *J. Adhesion* **3**, 145 (1971).
29. D. I. James, R. H. Norman and M. H. Stone, *Plastics & Polymers* **36**, 21 (1968).
30. R. H. Norman, M. H. Stone and W. C. Wake, *Glass Reinforced Plastics* Ed., B. Parkyn (Illiffe, London, 1970). P. 206.
31. R. A. Gledhill and A. J. Kinloch. Unpublished work.